# Numerical Study of the Combined Free-Forced Convection and Mass Transfer Flow Past a Vertical Porous Plate in a Porous Medium with Heat Generation and Thermal Diffusion

**M. S. Alam**[1], **M. M. Rahman**[2], **M. A. Samad**[3]

[1]Department of Mathematics, Dhaka University of Engineering and Technology
Gazipur-1700, Bangladesh
[2,3]Department of Mathematics, University of Dhaka, Dhaka-1000, Bangladesh
[2]mansurdu@yahoo.com

**Abstract.** The problem of combined free-forced convection and mass transfer flow over a vertical porous flat plate, in presence of heat generation and thermal-diffusion, is studied numerically. The non-linear partial differential equations and their boundary conditions, describing the problem under consideration, are transformed into a system of ordinary differential equations by using usual similarity transformations. This system is solved numerically by applying Nachtsheim-Swigert shooting iteration technique together with Runge-Kutta sixth order integration scheme. The effects of suction parameter, heat generation parameter and Soret number are examined on the flow field of a hydrogen-air mixture as a non-chemical reacting fluid pair. The analysis of the obtained results showed that the flow field is significantly influenced by these parameters.

**Keywords:** combined convection, mass transfer flow, heat generation, porous plate, numerical solution.

## 1 Introduction

It is known that a flow situation where both free and forced convection effects are of comparable order is called mixed convection. The study of such a mixed convection flow finds application in several industrial and technical processes such as nuclear reactors cooled during emergency shutdown, solar central receivers exposed to winds, electronic devices cooled by fans and heat exchangers placed

in a low-velocity environment. The simplest physical model of such a flow is the two dimensional laminar mixed convection flow along a vertical flat plate and extensive studies have been conducted on this type of flow [1–4]. Applications of this model can be found in the areas of reactor safety, combustion flames and solar collectors, as well as building energy conservation [5]. This model has also been used by many investigators to analyze the combined free-forced convective boundary layer flow, for micropolar fluids, or for the flow through porous media [6–12]. However, in the above studies mass diffusion due to temperature gradient, called thermal-diffusion has not been taken into account. Jha and Singh [13] and Kafoussias [14] have noted the importance of the effects of this thermal-diffusion. Recently Alam and Sattar [15] included the thermal-diffusion effect on MHD free convection and mass transfer flow. Very recently, Alam *et al.* [16] studied the above mention effect on unsteady MHD free convection and mass transfer flow past an impulsively started vertical porous plate. Hence, the objective of the present paper is to study the above mentioned thermal-diffusion effects as well as heat generation effects on steady combined free-forced convection and mass transfer flow past a semi-infinite vertical porous flat plate embedded in a porous medium. The volumetric heat generation term may exert a strong influence on the heat transfer and as a consequence, also on the fluid flow.

## 2   Mathematical analysis

A two-dimensional steady combined free-forced convective and mass transfer flow of a viscous, incompressible fluid over an isothermal semi-infinite vertical porous flat plate embedded in a porous medium is considered. The flow is assumed to be in the $x$-direction, which is taken along the vertical plate in the upward direction and the $y$-axis is taken to be normal to the plate. The surface of the plate is maintained at a uniform constant temperature $T_w$ and a uniform constant concentration $C_w$, of a foreign fluid, which are higher than the corresponding values $T_\infty$ and $C_\infty$, respectively, sufficiently far away from the flat surface. It is also assumed that the free stream velocity $U_\infty$, parallel to the vertical plate, is constant. The flow configuration is shown in the following Fig. 1.

Then under the boundary layer and Boussinesq's approximations, the gover-
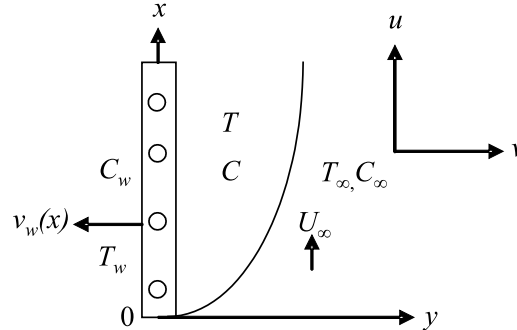
Fig. 1. Flow configuration and coordinate system.

ning equations are given by:

Continuity
$$\frac{\partial u}{\partial x} + \frac{\partial v}{\partial y} = 0, \tag{1}$$

Momentum
$$u\frac{\partial u}{\partial x} + v\frac{\partial u}{\partial y} = \nu\frac{\partial^2 u}{\partial y^2} + g\beta(T - T_\infty)$$
$$+ g\beta^*(C - C_\infty) - \frac{\nu}{K'}u, \tag{2}$$

Energy
$$u\frac{\partial T}{\partial x} + v\frac{\partial T}{\partial y} = \frac{k}{\rho c_p}\frac{\partial^2 T}{\partial y^2} + \frac{Q_0}{\rho c_p}(T - T_\infty), \tag{3}$$

Diffusion
$$u\frac{\partial C}{\partial x} + v\frac{\partial C}{\partial y} = D_M\frac{\partial^2 C}{\partial y^2} + D_T\frac{\partial^2 T}{\partial y^2}, \tag{4}$$

where $u, v$ are the velocity components in the $x$- and $y$- directions respectively, $\nu$ is the kinematic viscosity, $g$ is the acceleration due to gravity, $\rho$ is the density of the fluid, $\beta$ is the coefficient of volume expansion, $\beta^*$ is the volumetric coefficient of expansion with concentration, $T$, $T_w$ and $T_\infty$ are the temperature of the fluid inside the thermal boundary layer, the plate temperature and the fluid temperature in the free stream, respectively, while $C$, $C_w$ and $C_\infty$ are the corresponding concentrations. Also, $K'$ is the permeability of the porous medium, $k$ is the thermal conductivity, $c_p$ is the specific heat at constant pressure, $Q_0$ is the heat generation constant, $D_M$ is the coefficient of mass diffusivity and $D_T$ is the coefficient of thermal diffusivity.

For the flow there is no-slip at the plate. For uniform plate temperature and concentration the appropriate boundary conditions for the above problem are as

follows:

$$u = 0, \quad v = v_w(x), \quad T = T_w, \quad C = C_w \quad \text{at} \quad y = 0, \tag{5a}$$

$$u = U_\infty, \quad T = T_\infty, \quad C = C_\infty \quad \text{as} \quad y \to \infty. \tag{5b}$$

In order to obtain similarity solution of the problem we introduce the following non-dimensional variables (see Schlichting [17], Rahman and Sattar [18])

$$\eta = y\sqrt{\frac{U_\infty}{\nu x}}, \quad \psi = \sqrt{\nu x U_\infty} f(\eta),$$
$$\theta(\eta) = \frac{T - T_\infty}{T_w - T_\infty}, \quad \phi(\eta) = \frac{C - C_\infty}{C_w - C_\infty}, \tag{6a}$$

where $\psi$ is the stream function.

Since $u = \frac{\partial \psi}{\partial y}$ and $v = -\frac{\partial \psi}{\partial x}$ we have from equation (6a)

$$u = U_\infty f' \quad \text{and} \quad v = -\sqrt{\frac{\nu U_\infty}{x}}(f - \eta f'). \tag{6b}$$

Here prime denotes differentiation with respect to $\eta$.

Now substituting equation (6) in equations (2)–(4) we obtain

$$f''' + \frac{1}{2}ff'' - Kf' + g_s\theta + g_c\phi = 0, \tag{7}$$

$$\theta'' + \frac{1}{2}Pr f\theta' + Pr Q\theta = 0, \tag{8}$$

$$\phi'' + \frac{1}{2}Sc f\phi' + So Sc \theta'' = 0. \tag{9}$$

The boundary conditions (5) then turn into

$$f = f_w, \quad f' = 0, \quad \theta = 1, \quad \phi = 1, \quad \text{at} \quad \eta = 0, \tag{10a}$$

$$f' = 1, \quad \theta = 0, \quad \phi = 0, \quad \text{as} \quad \eta \to \infty, \tag{10b}$$

where $f_w = -2v_w(x)\sqrt{\frac{x}{\nu U_\infty}}$ is the suction parameter. The dimensionless parameters introduced in the above equations are defined as follows:

$$K = \frac{\nu x}{K' U_\infty} \quad \text{is the local Permeability parameter,}$$

$$Gr = \frac{g\beta(T_w - T_\infty)x^3}{\nu^2} \quad \text{is the local temperature Grashof number,}$$

$Gm = \dfrac{g\beta^*(C_w - C_\infty)x^3}{\nu^2}$    is the local mass Grashof number,

$Re = \dfrac{U_\infty x}{\nu}$    is the local Reynolds number,

$g_s = \dfrac{Gr}{Re^2}$   is the temperature buoyancy parameter,

$g_c = \dfrac{Gr}{Re^2}$   is the mass buoyancy parameter,

$Pr = \dfrac{\nu\rho c_p}{k}$   is the Prandtl number,

$Q = \dfrac{Q_0 x}{\rho c_p U_\infty}$   is the local heat generation parameter,

$Sc = \dfrac{\nu}{D_M}$   is the Schmidt number,

and   $So = \dfrac{D_T(T_w - T_\infty)}{\nu(C_w - C_\infty)}$   is the Soret number.

## 3   Numerical solutions

The system of non-linear ordinary differential equations (7)–(9) together with the boundary conditions (10) are locally similar and solved numerically using Nachtsheim-Swigert shooting iteration technique (guessing the missing value) along with sixth order Runge-Kutta initial value solver.

In a shooting method, the missing (unspecified) initial condition at the initial point of the interval is assumed, and the differential equation is then integrated numerically as an initial value problem to the terminal point. The accuracy of the assumed missing initial condition is then checked by comparing the calculated value of the dependent variable at the terminal point with its given value there. If a difference exists, another value of the missing initial condition must be assumed and the process is repeated. This process is continued until the agreement between the calculated and the given condition at the terminal point is within the specified degree of accuracy. For this type of iterative approach, one naturally inquires whether or not there is a systematic way of finding each succeeding (assumed) value of the missing initial condition.

The Nachtsheim-Swigert iteration technique thus needs to be discussed elaborately. The boundary conditions (10) associated with the non-linear ordinary

differential equations (7)–(9) are the two-point asymptotic class. Two-point boundary conditions have values of the dependent variable specified at two different values of independent variable. Specification of an asymptotic boundary condition implies that the first derivative (and higher derivatives of the boundary layer equations, if exist) of the dependent variable approaches zero as the outer specified value of the independent variable is approached.

The method of numerically integrating a two-point asymptotic boundary-value problem of the boundary-layer type, the initial-value method is similar to an initial-value problem. Thus it is necessary to estimate as many boundary conditions at the surface as were (previously) given at infinity. The governing differential equations are then integrated with these assumed surface boundary conditions. If the required outer boundary condition is satisfied, a solution has been achieved. However, this is not generally the case. Hence, a method must be devised to estimate logically the new surface boundary conditions for the next trial integration. Asymptotic boundary value problems such as those governing the boundary-layer equations are further complicated by the fact that the outer boundary condition is specified at infinity. In the trial integration infinity is numerically approximated by some large value of the independent variable. There is no a priori general method of estimating these values. Selecting too small a maximum value for the independent variable may not allow the solution to asymptotically converge to the required accuracy. Selecting large a value may result in divergence of the trial integration or in slow convergence of surface boundary conditions. Selecting too large a value of the independent variable is expensive in terms of computer time.

Nachtsheim-Swigert [19] developed an iteration method to overcome these difficulties. Extension of the Nachtsheim-Swigert iteration scheme to the system of equations (7)–(9) and the boundary conditions (10) is straightforward. In equation (10) there are three asymptotic boundary conditions and hence three unknown surface conditions $f''(0)$, $\theta'(0)$ and $\phi'(0)$.

Within the context of the initial-value method and Nachtsheim-Swigert iteration technique the outer boundary conditions may be functionally represented as

$$\Phi_j(\eta_{max}) = \Phi_j\big(f''(0), \theta'(0), \phi'(0)\big) = \delta_j, \quad j = 1, 2, \ldots, 6, \tag{11}$$

where $\Phi_1 = f'$, $\Phi_2 = \theta$, $\Phi_3 = \phi$, $\Phi_4 = f''$, $\Phi_5 = \theta'$, $\Phi_6 = \phi'$. The last three of these represents asymptotic convergence criteria.

Choosing $f''(0) = g_1$, $\theta'(0) = g_2$ and $\phi'(0) = g_3$ and expanding in a first-order Taylor's series after using equations (11) yield

$$\Phi_j(\eta_{max}) = \Phi_{j,C}(\eta_{max}) + \sum_{i=1}^{3} \frac{\partial \Phi_j}{\partial g_i} \Delta g_i = \delta_j, \quad j = 1, 2, \ldots, 6, \qquad (12)$$

where subscript 'C' indicates the value of the function at $\eta_{max}$ determined from the trial integration.

Solution of these equations in a least-square sense require determining the minimum value of

$$E = \sum_{j=1}^{6} \delta_j^2 \qquad (13)$$

with respect to $g_i$ $(i = 1, 2, 3)$.

Now differentiating $E$ with respect to $g_i$ we obtain

$$\sum_{j=1}^{6} \delta_j \frac{\partial \delta_j}{\partial g_i} = 0. \qquad (14)$$

Substituting equation (12) into (14) after some algebra we obtain

$$\sum_{k=1}^{3} a_{ik} \Delta g_k = b_i, \quad i = 1, 2, 3, \qquad (15)$$

where

$$a_{ik} = \sum_{j=1}^{6} \frac{\partial \Phi_j}{\partial g_i} \cdot \frac{\partial \Phi_j}{\partial g_k}, \quad b_i = -\sum_{j=1}^{6} \Phi_{j,C} \frac{\partial \Phi_j}{\partial g_i}, \quad i, k = 1, 2, 3. \qquad (16)$$

Now solving the system of linear equations (15) using Cramer's rule we obtain the missing (unspecified) values of $g_i$ as

$$g_i = g_i + \Delta g_i. \qquad (17)$$

Thus adopting the numerical technique aforementioned, the solution of the nonlinear ordinary differential equations (7)–(9) with boundary conditions (10) are obtained together with sixth-order Runge-Kutta initial value solver and determine the velocity, temperature and concentration as a function of the coordinate $\eta$.

## 4 Skin-friction coefficient, Nusselt number and Sherwood number

The parameters of engineering interest for the present problem are the local skin-friction coefficient, local Nusselt number and the local Sherwood number which indicate physically wall shear stress, rate of heat transfer and rate of mass transfer respectively.

The equation defining the wall skin-friction is

$$\tau_w = \mu\Big(\frac{\partial u}{\partial y}\Big)_{y=0} = \mu U_\infty \sqrt{\frac{U_\infty}{\nu x}}\, f''(0). \tag{18}$$

Hence the skin-friction coefficient is given by $C_f = \frac{2\tau_w}{\rho U_\infty^2}$ or

$$\frac{1}{2} C_f (Re)^{\frac{1}{2}} = f''(0). \tag{19}$$

Now the heat flux $(q_w)$ and the mass flux $(M_w)$ at the wall are given by

$$q_w = -k\Big(\frac{\partial T}{\partial y}\Big)_{y=0} = -k\Delta T \sqrt{\frac{U_\infty}{\nu x}}\, \theta'(0), \tag{20}$$

and

$$M_w = -D_M\Big(\frac{\partial C}{\partial y}\Big)_{y=0} = -D_M\Delta C \sqrt{\frac{U_\infty}{\nu x}}\, \phi'(0), \tag{21}$$

where $\Delta T = T_w - T_\infty$ and $\Delta C = C_w - C_\infty$.

Hence the Nusselt number $(Nu)$ and Sherwood number $(Sh)$ are obtained as $Nu = \frac{xq_w}{k\Delta T} = -(Re)^{\frac{1}{2}}\theta'(0)$ i.e.,

$$Nu(Re)^{-\frac{1}{2}} = -\theta'(0) \tag{22}$$

and $Sh = \frac{xM_w}{D_m\Delta C} = -(Re)^{\frac{1}{2}}\phi'(0)$ i.e.,

$$Sh(Re)^{-\frac{1}{2}}\phi'(0). \tag{23}$$

These above coefficients are then obtained numerically and are sorted in Table 1.

Table 1. Numerical values of $C_f$, $Nu$ and $Sh$ for $Pr = 0.71$, $Sc = 0.22$,
$g_s = 1.0$, $g_c = 0.1$ and $K = 0.05$

| $Q$ | $f_w$ | $So$ | $C_f$ | $Nu$ | $Sh$ |
|-----|-------|------|-------|------|------|
| 0.5 | 0.5 | 0.2 | 1.8022 | 0.1057 | 0.2893 |
| 1.0 | 0.5 | 0.2 | 2.3286 | -0.6636 | 0.3460 |
| 2.0 | 0.5 | 0.2 | 4.6052 | -5.1781 | 0.5962 |
| 2.0 | 1.0 | 0.2 | 4.5945 | -4.7310 | 0.6071 |
| 2.0 | 1.5 | 0.2 | 4.4999 | -4.1595 | 0.6119 |
| 2.0 | 1.5 | 0.8 | 4.5007 | -4.1846 | 1.1379 |
| 2.0 | 1.5 | 2.0 | 4.5056 | -4.1868 | 2.1804 |

## 5    Results and discussion

Numerical calculations have been carried out for different values of $f_w$, $Q$, and $So$ and for fixed values of $Pr$, $Sc$, $g_s$ and $g_c$. The value of $Pr$ is taken to be $0.71$ which corresponds to air and the value of $Sc$ is chosen to represent hydrogen at $25^0$ C and $1$ atm. The dimensionless parameter $g_s$ is used to represent the free, forced and combined (free-forced) convection regimes. The case $g_s \ll 1$ corresponds to pure forced convection, $g_s = 1$ corresponds to combined free-forced convection and $g_s \gg 1$ corresponds to pure free convection. As the local mass Grashof number is a measure of the buoyancy forces (due not temperature but to concentration differences) to the viscous forces, the dimensionless parameter $g_c$ has the same meaning as the parameter $g_s$. The non-dimensional parameter $g_s$, takes the value $0.1$ for low concentration. With the above-mentioned flow parameters, the results are displayed in Figs. 2–4, for the velocity, temperature and concentration profiles.

The effects of $f_w$ on the velocity field are shown in Fig. 2(a). It is seen from this figure that the velocity profiles decrease monotonically with the increase of suction parameter indicating the usual fact that suction stabilizes the boundary layer growth. The effects of $f_w$ on the temperature and concentration fields are displayed in Figs. 2(b) and 2(c) respectively. We see that both the temperature and concentration profiles decrease with the increase of $f_w$. Sucking decelerated fluid particles through the porous wall reduce the growth of the fluid boundary layer as well as thermal and concentration boundary layers.
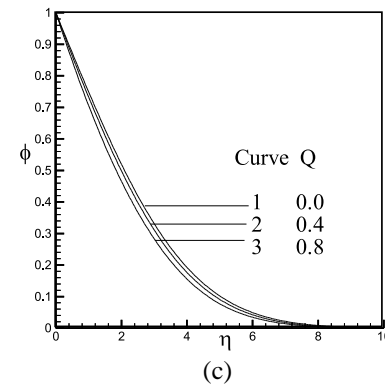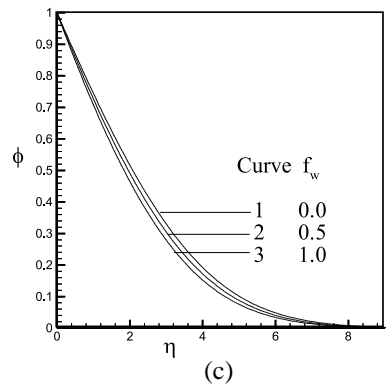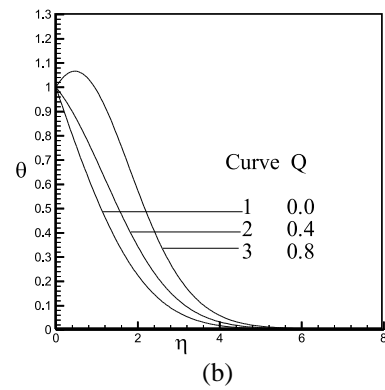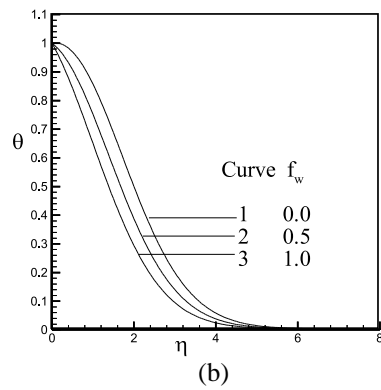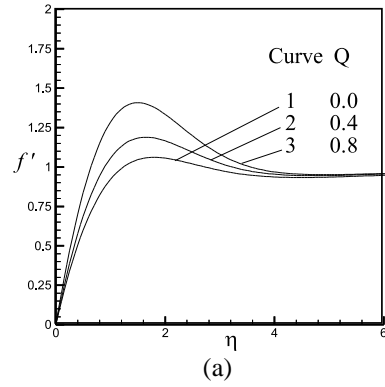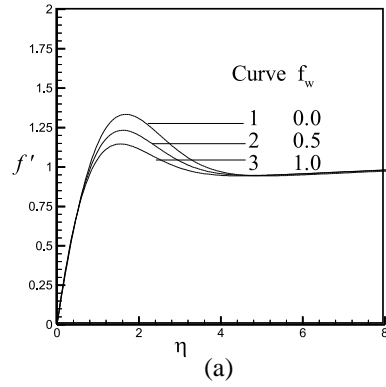
Fig. 2. Variations of (a) velocity, (b) temperature and (c) concentration across the boundary layer for $g_s = 1.0$, $g_c = 0.1$, $Pr = 0.71$, $Q = 0.5$, $Sc = 0.22$, $K = 0.05$ and $So = 0.2$.

Fig. 3. Variations of (a) velocity, (b) temperature and (c) concentration across the boundary layer for $g_s = 1.0$, $g_c = 0.1$, $Pr = 0.71$, $f_w = 0.5$, $Sc = 0.22$, $K = 0.05$ and $So = 0.2$.

The effect of $Q$ on the velocity profiles is shown in Fig. 3(a). From this figure we see that when the heat is generated the buoyancy force increases which induces the flow rate to increase giving rise to the increase in the velocity profiles. From Fig. 3(b), we observe that temperature increases significantly with the increase of $Q$. On the other hand, from Fig. 3(c) we see that the concentration profiles decrease with the increase of the heat generation parameter.

Fig. 4(a) shows the variation of dimensionless velocity profiles for different values of $So$. It is seen from this figure that velocity profiles increase with the increase of $So$ from which we conclude that the fluid velocity rises due to greater thermal-diffusion. Fig. 4(b) represents the concentration profiles for different values of $So$. From this figure we observe that the concentration profiles increase significantly with the increase of Soret number.
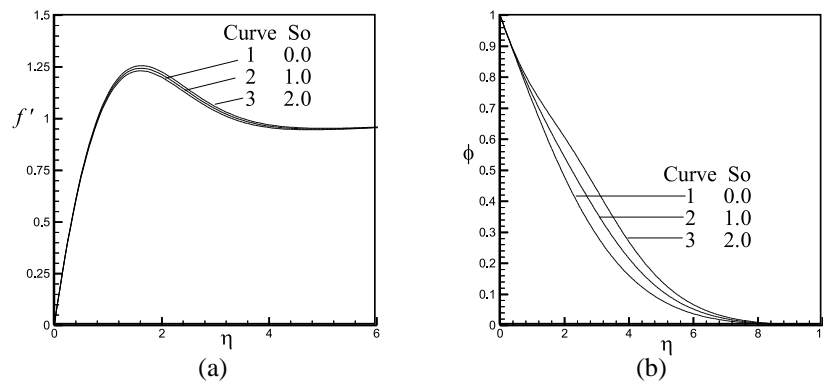


Fig. 4. Variations of (a) velocity and (b) concentration across the boundary layer for $g_s = 1.0$, $g_c = 0.1$, $Pr = 0.71$, $Q = 0.5$, $Sc = 0.22$, $K = 0.05$ and $f_w = 0.5$.

Finally the effects of the above-mentioned parameters on the skin-friction coefficients, Nusselt number and Sherwood number are shown in Table 1. The behavior of these parameters is self evident from Table 1 and hence any further discussions about them seem to be redundant.

## 6   Conclusions

In this paper we have studied numerically the steady two-dimensional combined free-forced convection and mass transfer flow over a semi-infinite vertical porous

plate embedded in a porous medium in presence of heat generation and thermal-diffusion. The effects of various parameters have been examined on the flow field for a hydrogen-air mixture as a non-chemical reacting fluid pair. From the present numerical investigation the following conclusions may be drown:

1. Wall suction stabilizes the velocity, thermal as well as concentration boundary layer growth.

2. Both the velocity and temperature profiles increase whereas the concentration profile decreases with the increase of heat generation parameter.

3. Both the velocity and concentration profiles increase with the increase of Soret number.

4. In mixed convection regime, both the Skin-friction coefficient and Sherwood number increases whereas the Nusselt number decreases with the increase of both heat generation parameter and Soret number.

## References

1. J. H. Merkin, The effects of buoyancy forces on the boundary layer flow over semi-infinite vertical flat plate in a uniform free stream, *J. Fluid Mech.,* **35**, pp. 439–450, 1969.

2. J. R. Lloyd, E. M. Sparrow, Combined forced and free convection flow on vertical surfaces, *Int. J. Heat Mass Transfer,* **13**(2), pp. 434–438, 1970.

3. G. Wilks, Combined forced and free convection flow on vertical surfaces, *Int. J. Heat Mass Transfer,* **16**(10), pp. 1958–1964, 1973.

4. M. S. Raju, X. R. Liu, C. K. Law, A formulation of combined forced and free convection past horizontal and vertical surfaces, *Int. J. Heat Mass Transfer,* **27**(12), pp. 2215–2224, 1984.

5. M. A. Hossain, M. U. Ahmed, MHD forced and free convection boundary layer flow near the leading edge, *Int. J. Heat Mass Transfer,* **33**(3), pp. 571–575, 1990.

6. A. Bejan, K. R. Khair, Heat and mass transfer by natural convection in a porous medium, *Int. J. Heat Mass Transfer,* **28**(5), pp. 909–918, 1985.

7. F. C. Lai, F. A. Kulacki, The effect of variable viscosity on convective heat transfer along a vertical surface in a saturated porous medium, *Int. J. Heat Mass Transfer,* **33**(5), pp. 1028–1031, 1990.

8. R. S. R. Gorla, P. P. Lin, A. J. Yang, Asymptotic boundary layer solutions for mixed convection from a vertical surface in a micropolar fluid, *Int. J. Eng. Sci.,* **28**(6), pp. 525–533, 1990.

9. O. V. Trevisan, A. Bejan, Combined heat and mass transfer by natural convection in a porous medium, *Adv. Heat Transfer,* **20**, pp. 315–352, 1990.

10. K. Tewari, P. Sing, Natural convection in a thermally stratified fluid saturated porous medium, *Int. J. Engng. Sci.,* **30**(8), pp. 1003–1007, 1992.

11. R. S. R. Gorla, Mixed convection in a micropolar fluid along a vertical surface with uniform heat flux, *Int. J. Eng. Sci.,* **30**(3), pp. 349–358, 1992.

12. S. D. Harris, D. B. Ingham, I. Pop, Unsteady mixed convection boundary layer flow on a vertical surface in a porous medium, *Int. J. Heat Mass Transfer,* **42**(2), pp. 357–372, 1999.

13. B. K. Jha, A. K. Singh, Soret effects free convection and mass transfer flow in the stokes problem for a infinite vertical plate, *Astrophysics and Space Science,* **173**(2), pp. 251–255, 1990.

14. N. G. Kafoussias, MHD Thermal-diffusion effects on free convective and mass transfer flow over an infinite vertical moving plate, *Astrophysics and Space Science,* **192**(1), pp. 11–19, 1992.

15. M. M. Alam, M. A. Sattar, Transient MHD heat and mass transfer flow with Thermal-diffusion in a rotating system, *J. Energy, Heat and Mass Transfer,* **21**, pp. 9–21, 1999.

16. M. S. Alam, M. M. Rahman, M. A. Maleque, Local similarity solutions for unsteady MHD free convection and mass transfer flow past an impulsively started vertical porous plate with Dufour and Soret effects, *Thammasat Int. J. Sci. Tech.,* **10**(3), pp. 1–8, 2005.

17. H. Schlichting, *Boundary layer theory,* 6th Edn. McGraw-Hill, New York, 1968.

18. M. M. Rahman, M. A. Sattar, Magnetohydrodynamic convective flow of a micropolar fluid past a continuously moving vertical porous plate in the presence of heat generation/absorption, *ASME J. Heat Trans.,* **128**(2), pp. 142–152, 2006.

19. P. R. Nachtsheim, P. Swigert, *Satisfaction of the asymptotic boundary conditions in numerical solution of the system of nonlinear equations of boundary layer type,* NASA TND-3004, 1965.